ACS Sustainable Chemistry & Engineering

Research Article

pubs.acs.org/journal/ascecg

Production of Acids and Bases for Ion Exchange Regeneration from Dilute Salt Solutions Using Bipolar Membrane Electrodialysis

Jake R. Davis, Yingying Chen, James C. Baygents, and James Farrell*

Department of Chemical and Environmental Engineering University of Arizona, 1133 E James E Rogers Way, Tucson, Arizona 85721, United States

Supporting Information

ABSTRACT: The acids and bases used for ion exchange regeneration contribute significantly to the increasing salinity of potable water supplies. This research investigated the use of bipolar membrane electrodialysis (BMED) for producing acids and bases from dilute salt solutions that are produced during reverse osmosis or evaporative cooling. Using single pass BMED, acids and bases were produced with concentrations equal to ∼75% of the feed salt concentration with current utilizations >75%. Current utilization increased with increasing feed salt concentrations due to decreased leakage current through the monopolar membranes. The maximum current density at which the BMED stack could be operated depended on the feed salt concentration and the flow velocity and was limited by water dissociation at the interface between the diluate solutions and the monopolar membranes. The stack resistance was dominated by the bipolar membranes, even for the most dilute feed solutions. The energy required per mole of acid or base produced increased linearly with increasing current density. The energy costs for producing acids and bases were significantly less than costs for purchasing bulk HCl and NaOH, and the process is scalable to large systems.

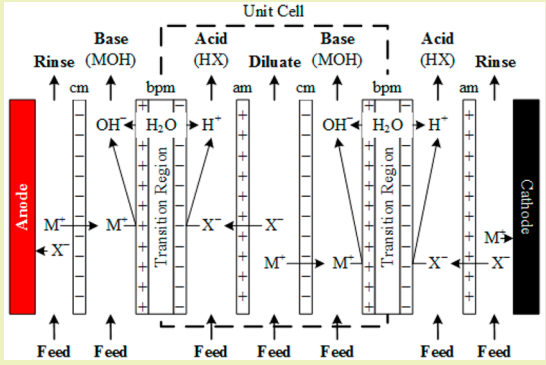

KEYWORDS: *Bipolar membrane electrodialysis, Ion exchange regeneration, Acid production, Water softening, Base production*

INTRODUCTION

Water softening is often used for producing water for use in electric power generation, evaporative cooling, and myriad other industrial processes. The most common method of industrial water softening is ion exchange, wherein scale forming ions, such as Ca^{2+} and Mg^{2+}, are removed via weak acid cation (WAC) ion exchange media containing weak acid anionic functional groups. The regeneration of WAC media requires large quantities of acids (e.g., HCl) and bases (e.g., NaOH), which after use, end up producing a brine stream. For example, a single regeneration cycle produces up to 320 kg of concentrated brine solution per cubic meter of ion exchange media.[1] These brines are a major contributor to the salinification of potable water supplies, especially in arid regions.[2] Conventional methods of brine disposal include discharge to the sea, deep-well injection, and metered discharge to the sewer system. Inland areas do not have the option of sea disposal and deep-well injection can be costly and must meet regulatory requirements.[3] Metered discharge to sewer systems can result in toxicity to biomass and inhibition of settling in clarifiers used in secondary wastewater treatment.[2]

The acids and bases needed for ion exchange media regeneration can be produced using an electrochemical cell and the ions that are already present in the water being treated. For example, bipolar membrane electrodialysis (BMED) can be used to generate acids and bases from the ions in cooling tower blowdown, or from reverse osmosis (RO) concentrates. Thus, onsite acid and base generation can eliminate the need for purchasing these chemicals while also eliminating the addition of salts to the water supply.

Bipolar Membrane Electrodialysis. The repeating unit cell in a BMED stack consists of an anion exchange membrane (AM), a bipolar membrane (BPM), and a cation exchange membrane (CM), as illustrated in Figure 1. BMED stacks may contain up to 300 of these repeating unit cells.[4] The BPM typically consists of three layers, a 50−100 μm thick strong acid CM, a ∼ 40 nm thick weak base layer, and a 50−100 μm thick strong base AM.[4] The weak base layer between the anion and cation membranes serves to promote the splitting of water into H^+ and OH^- ions via a catalytic mechanism and the second Wien effect.[4,5] Upon application of an electric field, H^+ ions created by water splitting migrate toward the cathode and get trapped in an acid chamber by an AM. Likewise, OH^- ions created by water splitting migrate toward the anode and get trapped in a base chamber by a CM. Electroneutrality is maintained in the acid chamber by electromigration of anions from the feed solution through the AM. In the base chamber, charge balance is maintained by cation migration from the feed solution through the CM.

Received: July 9, 2015
Revised: August 7, 2015
Published: August 18, 2015

DOI: 10.1021/acssuschemeng.5b00654
ACS Sustainable Chem. Eng. 2015, 3, 2337−2342

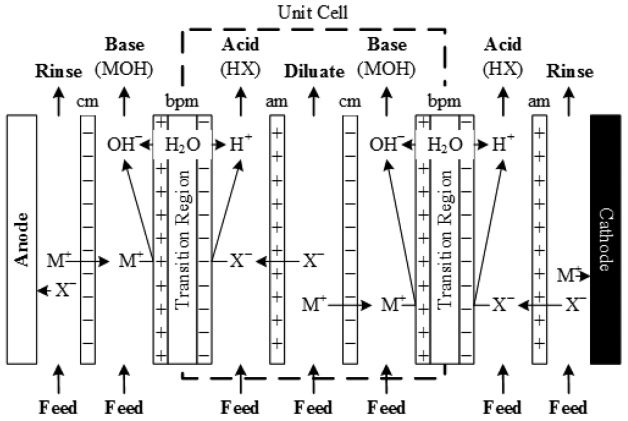

Figure 1. Schematic drawing illustrating the production of acids and bases from the corresponding salts by electrodialysis with bipolar membranes.

There are two limiting current densities (i) associated with BMED, one results from ion depletion in the bipolar membrane (i_{lim}^{BPM}), and the other is associated with the electrodialysis (ED) process occurring in the diluate compartment (i_{lim}^{ED}). The i_{lim}^{BPM} is reached when salt in the bipolar membrane is sufficiently depleted that it can no longer support the applied current.[6−11] Below i_{lim}^{BPM}, a significant portion of the current is carried across a bipolar membrane by salt diffusing into, and then electromigrating out of, the BPM. Above i_{lim}^{BPM}, the rate of salt ion electromigration out of the BPM is greater than the salt diffusion into the PBM. This results in increased resistance and enhanced water dissociation.[6−11] The i_{lim}^{ED} is caused by depletion of counterions adjacent to the AM or CM surfaces facing the diluate solution. As i_{lim}^{ED} is approached, the counterion concentration in the boundary layer becomes very low, causing the resistance of the boundary layer to drastically increase.[12−16] When i_{lim}^{ED} is reached, the counterion concentration is too low to carry the current through the adjacent monopolar membrane. This results in water splitting and drastically increases energy consumption.[12−16]

BMED operates on the same fundamental principles as electrodialysis (ED). However, these processes have different degrees of technical and commercial relevance, and are in different states of development. ED is a mature process with many applications in water desalination and in the food and drug industry. By contrast, BMED is an immature process that is more commonly used for processing and synthesis of high value commodities like wine and weak organic acids.[4,17]

The potential utility of BMED in water and wastewater treatment has long been recognized. Huang et al. investigated the use of BMED to regenerate a flue gas desulfurizing agent.[18] They found the process to be not only technically feasible but also economically attractive. Akse et al. considered BMED for on demand production of expendable reagents for use in advanced life support systems of next generation spacecraft.[19] Other research has investigated the recovery and purification of spent acids and bases.[20,21] In 1997, Mavrov et al. showed that BMED could be used to produce acids and bases from desalination brines used in membrane pretreatment processes.[22−25] However, Mavrov et al. did not investigate a range of feed salt concentrations and did not provide information needed to assess the Faradaic efficiencies and operational costs of using BMED in this application. The objectives of this research were to establish the basic relationships between the feed brine concentration, applied current density, energy consumption, membrane area, and reagent concentration. Each of these relationships is fundamental to an understanding of process economics and scalability.

MATERIALS AND METHODS

A block flow diagram of the experimental setup is shown in Figure 2. Feed solutions were prepared using ACS grade sodium chloride

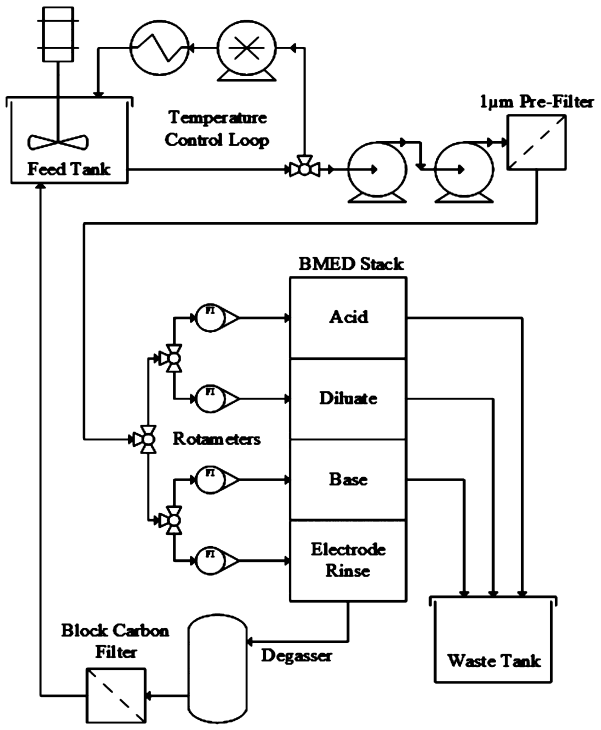

Figure 2. Block flow diagram of acid and base production process.

(NaCl), hydrochloric acid (HCl), and sodium hydroxide (NaOH) from Fisher Scientific, and 18 MΩ cm ultrapure water (UPW). The feed solution was contained in a continuously stirred 55 gallon high density polyethylene drum (HDPE) maintained at 25 °C using a stainless steel heat exchanger connected to a Laird MRC 300 chiller. The same feed solution passed through all compartments and was pumped using two Yamaha 80 W pool pumps placed in series. A 1 μm bag filter was placed prior to a manifold feeding four rotameters used for flow control. Experiments were conducted using the same flow rates for the acid base and diluate compartments. Total volumetric flow rates of 0.12 or 0.50 L min^{-1} were used for the acid, base and diluate solutions. The electrode rinse solution passed through both anode and cathode compartments at 1.5 L min^{-1}. After passing through the stack, the acid, base, and diluate streams were discharged to a second 55 gallon HPDE drum. The electrode rinse solutions were recirculated to the feed tank after passing through a custom degasser and a 10 in. long block carbon filter. The custom degasser was made from 1 in. PVC pipe and a float vent. The block carbon filter served to degrade hypochlorite formed via oxidation of Cl^- at the anode. The concentration of hypochlorite in the feed barrel was spot-checked using a pool test kit and never exceeded 0.5 mg L^{-1}, which was the minimum detection limit.

Acids and bases were produced during a single pass through a PC-Cell EDQ380 electrodialysis unit (PC-Cell GmbH, Heusweiler, Germany). The cell housing was made of polypropylene and had 380 cm^2 of active area per membrane. The stack contained 8 unit cells, consisting of a CM, a BPM, and an AM. Membrane spacers made of silicone rubber and polypropylene mesh were placed between each

DOI: 10.1021/acssuschemeng.5b00654
ACS Sustainable Chem. Eng. 2015, 3, 2337−2342

membrane pair forming 195 mm × 195 mm × 0.5 mm flow channels. The spacing between the electrodes and the cation exchange membranes terminating each end of the stack was approximately 2 mm. The cathode was made of an expanded stainless steel mesh and the anode was made of expanded titanium mesh with a platinum−iridium oxide coating. The anion exchange membrane (Neosepta ACM) was 0.17 mm thick and had an exchange capacity of 1.4−1.7 mequiv g^{-1}. The cation exchange membrane (Neosepta CMX) was 0.18 mm thick and had an exchange capacity of 1.5−1.8 mequiv g^{-1}. The bipolar membrane was a 0.22 mm thick Neosepta BP-1 bipolar membrane.

All acid and base production experiments were performed galvanostatically using a Xantrex XRT 40-21 power supply at cell currents between 1 and 10 A, corresponding to current densities ranging from 0.26 to 26 mA cm^{-2}. Samples were simultaneously drawn from the acid, base, dilute, feed, and electrode wash streams. The pH, conductivity, and temperature of each sample was measured using an AquaPro 9156APWP epoxy body pH probe, an Accument two-cell conductivity and temperature sensor, and a Symphony model SB90M5 multimeter. All probes were calibrated daily. Before samples were taken, the BMED stack was given a minimum of 10 min to come to steady state, equivalent to between 8 and 33 bed volumes. The approach to steady state was monitored with current and potential readings taken every minute.

Sodium concentrations in the feed, diluate, acid and base solutions were determined using a PerkinElmer Optima 2100 DV inductively coupled plasma optical emission spectrophotometer (ICP-OES). Samples were analyzed in triplicate at 589.592 nm. The acid and base concentrations were determined using pH measurements with activity coefficient corrections using the Pitzer model,[26] and the measured Na^+ concentration and pH of each sample.

RESULTS AND DISCUSSION

The first research task was to determine the effect of feed salt concentration on the highest acid and base concentrations that could be made without exceeding the limiting current density in the diluate compartment, i_{lim}^{ED}. Figure 3 shows the acid and base concentrations as a function of current density produced from NaCl solutions ranging from 48 mM to 390 mM using flow velocities of 0.25 and 1.2 cm s^{-1}. The maximum acid and base concentrations that could be achieved for each feed solution are listed in Table 1. Also listed in Table 1 is the fraction of the maximum possible acid and base concentrations that could be

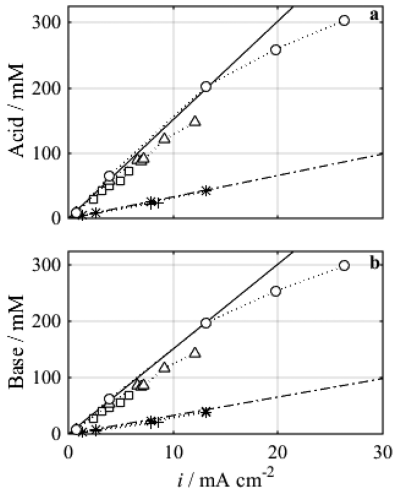

Figure 3. Concentration of acid (**a**) or base (**b**) made from 48 mM (crosses), 95 mM (squares), 118 mM (asterisks), 192 mM (triangles), and 390 mM (circles) sodium chloride solutions, flowing at 1.2 cm s^{-1} (linear markers) or 0.25 cm s^{-1} (geometric markers), as a function of current density (i). The solid line illustrates $\xi_i = 1$ for $u = 0.25$ cm s^{-1} and the dot dashed line illustrates $\xi_i = 1$ for $u = 1.2$ cm s^{-1}.

Table 1. Maximum Acid and Base Concentrations for Different Feed Solution NaCl Concentrations (C), Limiting Current Densities (i_{lim}^{ED}), and Fraction of Maximum Possible Concentrations for Acid and Base Production

C (mM)	i_{lim}^{ED} (mA cm^{-2})	acid (mM)	base (mM)
48	3.2	39/81%	37/77%
95	5.8	73/77%	69/73%
192	12.1	148/77%	144/75%
390	26.3	303/78%	299/77%

obtained from each feed solution without co-ion transport through the monopolar membranes. The fraction of the maximum concentrations that were attained based on the feed solution concentrations ranged from 77 to 81% for acids, and 73 to 77% for base. To produce these acids and bases required removing ∼75% of the Na^+ and Cl^- ions from the feed solutions passing through the diluate chamber. For the 236 mM feed solution at 1.2 cm s^{-1}, it was not possible to determine the maximum acid and base concentration due to the 40 V limit on the power supply.

The solid line in Figure 3 illustrates the maximum possible acid and base concentrations that could be produced for 100% current utilization (ξ), which is equivalent to the Faradaic efficiency for acid and base production. The current utilization can be determined from

$$\xi = \frac{FCQ}{nI} \quad (1)$$

where F is Faraday's constant, C is the acid or base normality (i.e., concentration in equivalents per liter), Q is the volumetric flow rate of acid or base, I is the applied current, and n is the number of unit cells (i.e., 8). The ξ values for acid and base production with u = 0.25 cm s^{-1} are shown in Figure 4. At

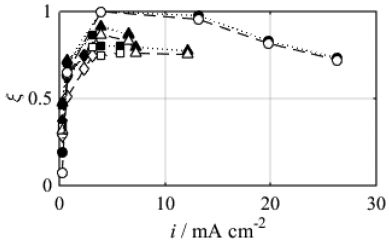

Figure 4. Acid (closed markers) and base (open markers) current utilization (ξ), made from 48 mM (diamonds), 95 mM (squares), 192 mM (triangles), and 390 mM (circles) sodium chloride solutions flowing at 0.25 cm s^{-1}, as a function of current density (i).

current densities less than 2 mA cm^{-2}, ξ values less than 75% are the result of $i < i_{lim}^{BPM}$. In this circumstance, there was substantial diffusion of Na^+ and Cl^- back into the transition region against the electric field. Electromigration of these ions out of the transition region decreased the current associated with water splitting. At current densities greater than 2 mA cm^{-2}, current utilization less than 100% can be attributed to leakage of acid and base across the monopolar membranes, and to the splitting of water at the diluate−monopolar membrane interface. Leakage of base into the diluate compartments was experimentally observed by slight increases in pH for the

DOI: 10.1021/acssuschemeng.5b00654
ACS Sustainable Chem. Eng. 2015, 3, 2337−2342

diluate solution, but never by more than 5 mM. There was also some acid leakage into the diluate compartment, but it was less than the base leakage; consequently, acid concentrations and ξ values were always slightly higher than those for the corresponding base, as shown in Figure 4. The fraction of the acid and base that leaked into the diluate compartment decreased with increasing concentration of the feed solution, as illustrated in Figure 4 by the increasing ξ values with increasing feed concentration. This occurred because greater salt concentrations in the acid and base allowed a greater fraction of the co-ion leakage currents to be carried by Na^+ and Cl^-, rather than H^+ and OH^-, for a given acid and base concentration. Similar conclusions can be made for the data taken with u = 1.2 cm s^{-1}, as shown in Figure S1 in the Supporting Information.

The effect of i_{lim}^{ED} on ξ values at 0.25 cm s^{-1} can be seen in Figure 4. For each feed concentration, there was a drop in ξ value when i_{lim}^{ED} was exceeded. These drops are due to the onset of field enhanced water dissociation at the monopolar membrane-diluate solution interfaces.[15,4,27,28] This transition to a current limited regime manifests as a sharp increase in stack resistance. The change in stack resistance occurs when the counterion concentration at the ion exchange membrane-diluate solution interface approaches zero.[15,4,27,28] Transitions to a current limited regime are commonly identified by constructing a resistance per unit cell (R) versus inverse current plot,[12] as shown in Figure 5. These transitions manifest as

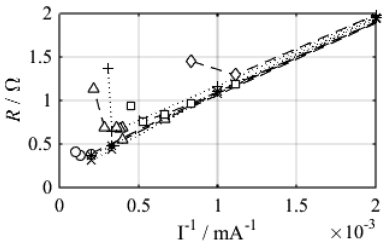

Figure 5. Resistance of a unit cell (R) as a function of inverse current (I^{-1}) for 48 mM (diamonds), 49 mM (pluses), 95 mM (squares), 118 mM (exes), 192 mM (triangles), 236 mM (asterisks), and 390 mM (circles) sodium chloride solutions for u = 0.25 cm s^{-1} (linear markers) and u = 1.2 cm s^{-1} (geometric markers).

sudden increases in R with increasing current, i.e. decreasing inverse current (I^{-1}). The abrupt drop in ξ values seen in the acid and base production data coincide with transitions to current limited regimes. The i_{lim}^{ED} was exceeded in every 0.25 cm s^{-1} data set and in the 48 mM feed solution flowing at 1.2 cm s^{-1}. The magnitude of i_{lim}^{ED} increased with increasing feed salt concentration and increasing diluate flow velocity. This dependence of i_{lim}^{ED} on flow velocity and diluate salt concentration is indistinguishable from that in ED without bipolar membranes.[12,14−16]

Figure 5 also demonstrates that the stack resistance was dominated by the resistance of the bipolar membranes, which were, to a first approximation, only dependent on current density. The acid, base, and diluate solutions, the CM, BPM, and AM, represent series resistances within a BMED stack. Bulk solution resistance is dependent on salt concentration. The resistance of the laminar boundary layer adjacent to the monopolar membranes is dependent on bulk solution concentration and flow velocity, and the resistance of the monopolar membranes is, to a first approximation, constant. The data in Figure 5 shows that the stack resistance was essentially independent of solution composition and flow velocity for $i < i_{lim}^{ED}$. The resistance of bipolar membranes is known to decrease with increasing current density.[9,10] Thus, the trend in Figure 5 shows that the resistance of the stack was controlled almost entirely by the resistance of the BPM.

Energy Utilzation. The energy requirements (E) for producing a mole of acid or base can be determined from the ratio of the applied power (I^2R) to the molar production rate of acid or base ($\xi nI/F$), as given by

$$E = \frac{1/2IRF}{n\xi} \quad (2)$$

Equation 2 attributes half the energy for acid production and half the energy for base production, since they are produced simultaneously. Figure 6a shows the E values for both acid and

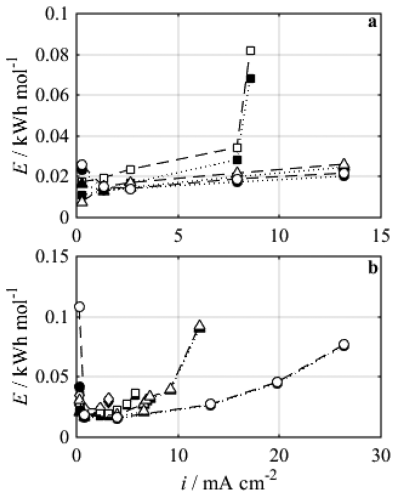

Figure 6. (a) Acid (closed markers) and base (open markers) molar energy (E) requirement, made from 49 mM (squares), 118 mM (triangles), and 236 mM (circles) sodium chloride solutions flowing at 1.2 cm s^{-1}, as a function of current density (i). (b) Acid (closed markers) and base (open markers) molar energy (E), made from 48 mM (diamonds), 95 mM (squares), 192 mM (triangles), and 390 mM (circles) sodium chloride solutions flowing at 0.25 cm s^{-1}, as a function of current density (i).

base production as a function of current density for a fluid velocity of 1.2 cm s^{-1}. The data set for a feed NaCl concentration of 49 mM shows the effect of exceeding i_{lim}^{ED} on the molar energy requirements. For this feed solution, i_{lim}^{ED} was exceeded for i > 8 mA cm^{-2}. In the other feed solutions, i_{lim}^{ED} was not exceeded, and E values increased linearly with i once i_{lim}^{BPM} was reached, in accord with eq 2. For current densities between i_{lim}^{ED} and i_{lim}^{BPM}, both R and ξ were dependent on current density. Figure S2 in the Supporting Information shows that R decreases with increasing current density, and Figure 4 shows the effect of current density on ξ values. Thus, the linear relationship between E and i results from cancellation of these two opposing effects. The data in Figure 6b shows the effect of current density on E values for a fluid velocity of 0.25 cm s^{-1}. For all feed concentrations, i_{lim}^{BPM} was reached or exceeded, and the energy requirements ranged from 0.02 to 0.09 kW h mol^{-1}.

Scalability. The size of the BMED cell that is needed for a particular application will depend on the current density at which it can be operated. This current density is dependent on the salt concentration of the feed solution and the linear

DOI: 10.1021/acssuschemeng.5b00654
ACS Sustainable Chem. Eng. 2015, 3, 2337−2342

velocity in the cell, because of boundary layer mass transfer effects. For an RO concentrate with 90% recovery, the ionic strength of the concentrate solution will be 10 times the concentration of the feed solution, which is typically ~10−12 mN. Thus, the data in Figure 6a for a 118 mN feed solution can be used to estimate the BMED stack size required for producing sufficient acid or base for regenerating ion exchange media per volume of water softened. When operated at 13.2 mA cm^{-2} the ξ value for acid production is 98% (Figure S1). This results in an acid production rate of 116 mol d^{-1} m^{-2} of active membrane area. To put this number in perspective, the membrane area required for producing enough acid to regenerate WAC media with a feed hardness of 4 mequiv L^{-1} can be calculated per million gallons of water treated per day (MGD). Based on stoichiometric regeneration of the WAC media,[29] 15.1 kmol d^{-1} of acid and base are required per MGD of water softened. Thus, the membrane area required is 130 m^2 per MGD of water softened. Commercial BMED stacks often contain more than 100 unit cells each with an active membrane area of 1 m^2 or more.[4] Thus, approximately 1 commercial BMED stack would be sufficient for supplying acid and base for softening 1 MGD of water with 4 mequiv L^{-1} of hardness.

The range of E values for current densities >5 mA cm^{-2} (0.025 to 0.09 kWh mol^{-1}) in Figure 6 can be used to estimate the energy costs for acid and base production under practical conditions. Assuming an industrial energy cost of $0.07 kW^{-1} h^{-1},[30] the cost to make 1 kmol of acid and base ranges from $1.75 to $6.30, exclusive of pumping costs. The pumping costs are typically similar to those for operating the BMED stack.[4] These values can be compared to the costs for purchasing acids and bases in large quantities. Table 2 shows current cost estimates for purchasing HCl and NaOH in bulk quantities, including freight costs, which typically run about $100/ton.[31,32] Also shown in Table 2 are the range in electrical energy costs, including pumping, for onsite acid and base generation. At all current densities and flow velocities, the costs for making acids and bases was significantly lower than purchasing acids and bases in multiple ton quantities.

Table 2. Cost Comparison for Purchasing Bulk HCl and NaOH Compared with Energy Cost for Onsite Generation, Assuming Electrical Energy Priced at $0.07 kW^{-1} h^{-1}[a]

chemical	purchase cost[31,32] ($ ton^{-1})	purchase cost ($ $kmol^{-1}$)	BMED cost ($ $kmol^{-1}$)
35% HCl	320	37	3.5−12.6
99% NaOH	525	21	3.5−12.6

[a]A freight cost of $100/ton was added to the purchased reagents. The BMED energy cost includes the electrical energy to run the BMED cell and electrical pumping cost, which is assumed equivalent to the cost to operate the cell.

A more thorough analysis of the total operating costs would require many assumptions that would be heavily dependent on the application. However, a rough estimate can be made from a previously published analysis for making 2 N acid and base solutions from a 2.5 N NaCl solution.[4] This analysis indicates that the total costs for acid and base production are 1.7 times the energy cost, assuming a current utilization of 70%. The total costs include all peripheral equipment, maintenance, cost of capital, and membrane replacement every two years. Thus, even when these costs are included, the process proposed here remains cost competitive to purchasing acids and bases. However, the cost for purchasing acids and bases does not include the environmental cost of increasing the salinity of the water supply.

This research showed that dilute salt solutions can be used to make acids and bases cost-effectively with high Faradaic efficiencies. The lowest salt concentration investigated (48 mM), typical of that in an evaporative cooling system operating at 5 cycles of concentration, can make acid sufficiently strong to regenerate WAC ion exchange media. The ion exchange media can be used to soften the water and remove other multivalent cations that may foul the BMED stack prior to use in the cooling system. Softened water in evaporative cooling systems will eliminate the need for adding scale inhibiting chemicals and will also allow the cooling system to be operated at higher cycles of concentration, thereby saving on water use. Water softening prior to reverse osmosis will also eliminate the need for adding scale inhibitors and will result in water savings by allowing higher permeate recoveries. Making ion exchange regenerant solutions from ions that are present in the feedwater will greatly reduce the impact of ion exchange softening on the salinification of potable water supplies.

■ ASSOCIATED CONTENT

Supporting Information

The Supporting Information is available free of charge on the ACS Publications website at DOI: 10.1021/acssuschemeng.5b00654.

Figures showing the current utilization for acid and base production for NaCl solutions flowing at 1.2 cm s^{-1} and the unit cell resistance as a function of current density (PDF)

■ AUTHOR INFORMATION

Corresponding Author

*E-mail: farrellj@email.arizona.edu. Tel.: 520 940-0487.

Notes

The authors declare no competing financial interest.

■ ACKNOWLEDGMENTS

The National Science Foundation (CBET-1235596) provided funding for this work.

■ REFERENCES

(1) American Water Works Association. *Water Quality and Treatment*, 5th ed.; McGraw Hill: New York, 1999.

(2) *Central Arizona Salinity Study, Phase II, Final Report*; U.S. Bureau of Reclamation: Washington, DC, 2006.

(3) Pérez-González, A.; Urtiaga, A. M.; Ibáñez, R.; Ortiz, I. State of the art and review on the treatment technologies of water reverse osmosis concentrates. *Water Res.* **2012**, *46*, 267−283.

(4) Strathmann, H. *Ion-Exchange Membrane Separation Processes*; Elsevier: Amsterdam, 2004.

(5) Onsager, L. Deviations from Ohm's law in weak electrolytes. *J. Chem. Phys.* **1934**, *2*, 599−615.

(6) Tanioka, A.; Shimizu, K.; Hosono, T.; Eto, R.; Osaki, T. Effect of interfacial state in bipolar membrane on rectification and water splitting. *Colloids Surf., A* **1999**, *159*, 395−404.

(7) Xue, Y.; Xu, T.; Fu, R.; Cheng, Y.; Yang, W. Catalytic water dissociation using hyperbranched aliphatic polyester (Boltorn® series) as the interface of a bipolar membrane. *J. Colloid Interface Sci.* **2007**, *316*, 604−611.

(8) Mafé, S.; Ramírez, P.; Alcaraz, A.; Mafe, S.; Ramırez, P. Electric field-assisted proton transfer and water dissociation at the junction of a fixed-charge bipolar membrane. *Chem. Phys. Lett.* **1998**, *294*, 406−412.

DOI: 10.1021/acssuschemeng.5b00654
ACS Sustainable Chem. Eng. 2015, 3, 2337−2342

(9) Simons, R.; Khanarian, G. Water dissociation in bipolar membranes: experiments and theory. *J. Membr. Biol.* **1978**, *38*, 11−30.
(10) Strathmann, H.; Krol, J. J.; Rapp, H. J.; Eigenberger, G. Limiting current density and water dissociation in bipolar membranes. *J. Membr. Sci.* **1997**, *125*, 123−142.
(11) Alcaraz, A.; Ramırez, P.; Mafe, S.; Holdik, H.; Bauer, B. Ion selectivity and water dissociation in polymer bipolar membranes studied by membrane potential and current−voltage measurements. *Polymer* **2000**, *41*, 6627−6634.
(12) Lee, H. J.; Strathmann, H.; Moon, S. H. Determination of the limiting current density in electrodialysis desalination as an empirical function of linear velocity. *Desalination* **2006**, *190*, 43−50.
(13) Tanaka, Y. Mass transport in a boundary layer and in an ion exchange membrane: Mechanism of concentration polarization and water dissociation. *Russ. J. Electrochem.* **2012**, *48*, 665−681.
(14) Silva, V.; Poiesz, E.; Heijden, P. Industrial wastewater desalination using electrodialysis: evaluation and plant design. *J. Appl. Electrochem.* **2013**, *43*, 1057−1067.
(15) Krol, J. J.; Wessling, M.; Strathmann, H. Concentration polarization with monopolar ion exchange membranes: current−voltage curves and water dissociation. *J. Membr. Sci.* **1999**, *162*, 145−154.
(16) Lee, J. W.; Yeon, K.-H.; Song, J.-H.; Moon, S.-H. Characterization of electroregeneration and determination of optimal current density in continuous electrodeionization. *Desalination* **2007**, *207*, 276−285.
(17) Bazinet, L.; Lamarche, F.; Ippersiel, D. Bipolar-membrane electrodialysis: applications of electrodialysis in the food industry. *Trends Food Sci. Technol.* **1998**, *9*, 107−113.
(18) Huang, C.; Xu, T.; Jacobs, M. L. Regenerating flue-gas desulfurizing agents by bipolar membrane electrodialysis. *AIChE J.* **2006**, *52*, 393−401.
(19) *On demand electrochemical production of reagent to minimize resupply of expendables*; UMPQUA Research Company Report 1999-01-2181; UMPQUA Research Company: Myrtle Creek, OR, 1999; http://www.urc.cc/pubs/URC-1999b.pdf.
(20) Chiao, Y. C.; Chlanda, F. P.; Mani, K. N. Bipolar membranes for purification of acids and bases. *J. Membr. Sci.* **1991**, *61*, 239−252.
(21) Mani, K. N.; Chlanda, F. P.; Byszewski, C. H. Aquatech membrane technology for recovery of acid/base values for salt streams. *Desalination* **1988**, *68*, 149−166.
(22) Mavrov, V.; Chmiel, H.; Heitele, B.; Rögener, F.; Riigener, F. Desalination of surface water to industrial water with lower impact on the environment. Part 1: New technological concept. *Desalination* **1997**, *108*, 159−166.
(23) Mavrov, V.; Chmiel, H.; Heitele, B.; Rögener, F. Desalination of surface water to industrial water with lower impact on the environment. Part 2: Improved feed water pretreatment. *Desalination* **1997**, *110*, 65−73.
(24) Mavrov, V.; Chmiel, H.; Heitele, B.; Rögener, F. Desalination of surface water to industrial water with lower impact on the environment Part 3: Water desalination under alkaline conditions. *Desalination* **1999**, *123*, 33−43.
(25) Mavrov, V.; Chmiel, H.; Heitele, B.; Rögener, F. Desalination of surface water to industrial water with lower impact on the environment: Part 4: Treatment of effluents from water desalination stages for reuse and balance of the new technological concept for water desalination. *Desalination* **1999**, *124*, 205−216.
(26) Pitzer, K. S. *Activity Coefficients in Electrolyte Solutions*; CRC Press: Boca Raton, FL, 1991.
(27) Mavrov, V.; Pusch, W.; Wheelwright, S.; Kominek, O. Concentration polarization and water splitting at electrodialysis membranes. *Desalination* **1993**, *91*, 225−252.
(28) Rubinstein, I.; Warshawsky, A.; Schechtman, L.; Kedem, O. Elimination of acid-base generation ("water-splitting") in electrodialysis. *Desalination* **1984**, *51*, 55−60.
(29) Bornak, W. E. *Ion Exchange Deionization*; Tall Oaks Publishing: Littleton, CO, 2003.
(30) Electricity Data Browser. http://www.eia.gov/electricity/data/browser/#/topic/7?agg=2,0,1&geo=g&freq=M (accessed Dec 5, 2014).
(31) ICIS. http://www.icis.com/resources/news/2014/11/03/9834809/us-hcl-market-range-grows-on-short-supply-and-high-prices/ (accessed Dec 5, 2014).
(32) ChemCenters.com. http://www.chemcenters.com/159839 (accessed Dec 5, 2014).

DOI: 10.1021/acssuschemeng.5b00654
ACS Sustainable Chem. Eng. 2015, 3, 2337−2342